Title: Temperature drives variation in flying insect biomass across a German malaise trap network

Running head: Insect biomass over ecological gradients

Authors: Ellen A.R. Welti[1]*, Petr Zajicek[1], Manfred Ayasse[2], Tim Bornholdt[3], Jörn Buse[4], Frank Dziock[5], Rolf A. Engelmann[6,7], Jana Englmeier[8], Martin Fellendorf[2], Marc I. Förschler[4], Mark Frenzel[9], Ute Fricke[10], Cristina Ganuza[10], Mathias Hippke[11], Günter Hoenselaar[12], Andrea Kaus-Thiel[13], Klaus Mandery[14], Andreas Marten[15], Michael T. Monaghan[16,17], Carsten Morkel[12], Jörg Müller[8], Stephanie Puffpaff[18], Sarah Redlich[10], Ronny Richter[6,7,19], Sandra Rojas Botero[20], Tobias Scharnweber[21], Gregor Scheiffarth[22], Paul Schmidt Yáñez[16], Rhena Schumann[23,24], Sebastian Seibold[25,26], Ingolf Steffan-Dewenter[10], Stefan Stoll[27], Cynthia Tobisch[28], Sönke Twietmeyer[29], Johannes Uhler[8], Juliane Vogt[20], Dirk Weis[30], Wolfgang W. Weisser[20], Martin Wilmking[21], Peter Haase[1,31]

Author affiliations:

[1] Department of River Ecology and Conservation, Senckenberg Research Institute and Natural History Museum Frankfurt, Gelnhausen 63571 Germany

[2] Institute of Evolutionary Ecology and Conservation Genomics, Ulm University, Ulm 89075 Germany

[3] Lower Oder Valley National Park, Schwedt/Oder, OT Criewen 16303 Germany

[4] Black Forest National Park, Freudenstadt 72250 Germany

[5] Animal Ecology, University of Applied Sciences HTW Dresden, Pillnitzer Platz 2, Dresden 01326 Germany

[6] German Centre for Integrative Biodiversity Research (iDiv), Halle-Jena-Leipzig, Leipzig 04103 Germany

[7] Systematic Botany and Functional Biodiversity, Institute for Biology, Leipzig University, Berlin 04103 Germany

[8] Ecological Field Station, University of Würzburg, Rauhenebrach 96181 Germany

[9] Community Ecology, Helmholtz Centre for Environmental Research, Halle 06120 Germany

[10] Animal Ecology and Tropical Ecology, Biocenter, University of Würzburg, Würzburg 97074 Germany

[11] Biosphärenreservatsamt Schaalsee-Elbe, Zarrentin am Schaalsee 19246 Germany

[12] Kellerwald-Edersee National Park, Bad Wildungen 34537 Germany

[13] Hunsrück-Hochwald National Park, Birkenfeld 55765 Germany

[14] Institut für Biodiversitätsinformation e.V., Ebern 96106 Germany

[15] Harz National Park, Wernigerode 38855 Germany

[16] Leibniz Institute of Freshwater Ecology and Inland Fisheries (IGB), Berlin 12587 Germany

[17] Institut für Biologie, Freie Universität Berlin, 14195 Germany

[18] Nationalparkamt Vorpommern, Born a. Darß 18375 Germany

[19] Geoinformatics and Remote Sensing, Institute for Geography, Leipzig University, Leipzig 04103 Germany

[20] Restoration Ecology Research Group, Department of Ecology and Ecosystem Management, Technical University of Munich, Freising 85354 Germany

[21] Institute for Botany and Landscape Ecology, University Greifswald, Greifswald 17489 Germany

[22] Lower Saxon Wadden Sea National Park Authority, Wilhelmshaven 26382 Germany

[23] Biological Station Zingst, University of Rostock, Zingst 18374 Germany

[24] Mathematics and Natural Sciences, Institute of Biological Science, University of Rostock, Rostock 18059 Germany

[25] Ecosystem Dynamics and Forest Management Research Group, Technical University of Munich, Freising 85354 Germany

[26] Berchtesgaden National Park, Berchtesgaden 83471 Germany

[27] Environmental Planning and Technology, University of Applied Sciences Trier, Environmental Campus Birkenfeld, Birkenfeld 55761 Germany

[28] Institute for Ecology and Landscape, Weihenstephan University of Applied Sciences, Freising 85354 Germany

[29] Eifel National Park, Schleiden-Gemünd 53937 Germany

[30] Biosphärenreservat Oberlausitzer Heide- und Teichlandschaft, Malschwitz OT Wartha 02694 Germany

[31] Faculty of Biology, University of Duisburg-Essen, Essen, Germany

*corresponding author, email: ellen.welti@senckenberg.de

ABSTRACT

1) Among the many concerns for biodiversity in the Anthropocene, recent reports of flying insect loss are particularly alarming, given their importance as pollinators and as a food source for many predators. Few insect monitoring programs cover large spatial scales required to provide more generalizable estimates of insect responses to global change drivers.

2) We ask how climate and surrounding habitat affect flying insect biomass and day of peak biomass using data from the first year of a new standardized distributed monitoring network at 84 locations across Germany comprising spatial gradient of land-cover types from protected to urban areas.

3) Flying insect biomass increased linearly with monthly temperature across Germany. However, the effect of temperature on flying insect biomass flipped to negative in the hot months of June and July when local temperatures most exceeded long-term averages.

4) Land-cover explained little variation in insect biomass, but biomass was lowest in forested sites. Grasslands, pastures and orchards harbored the highest insect biomass. The date of peak biomass was primarily driven by surrounding land-cover type, with grasslands especially having earlier insect biomass phenologies.

5) Standardized, large-scale monitoring is pivotal to uncover underlying processes of insect decline and to develop climate-adapted strategies to promote insect diversity. In a temperate climate region, we find that the benefits of temperature on flying insect biomass diminish in a German summer at locations where temperatures most exceeded long-term averages. These results highlighting the importance of local adaptation in climate change-driven impacts on insect communities.

Keywords: ecological gradients, climate change, land-cover, insect monitoring, malaise trap, pollinator, thermal performance, LTER

INTRODUCTION

Insects constitute much of terrestrial biodiversity and deliver essential ecosystem services such as pollination of the majority of wild plants and 75% of crop species (Losey & Vaughan, 2006; Vanbergen & Insect Pollinators Initiative, 2013). Insect biomass is a key constituent of energy flows in many food webs (Stepanian et al., 2020), a useful measure of whole insect communities (Shortall et al., 2009) and an indicator of ecosystem function (Barnes et al., 2016; Dangles et al., 2011). Climate change and anthropogenically-altered land-cover are likely drivers of insect declines, but their effects on insect biomass are still poorly characterized (Habel et al., 2019). Amidst burgeoning evidence of widespread insect declines, standardized, and large scale insect monitoring is needed to improve estimates of trends, and identify drivers (Didham et al., 2020; Wagner, 2020).

Climate change is geographically pervasive (Wilson & Fox, 2020) and may explain insect decline in natural areas (e.g. Janzen & Hallwachs, 2019; Welti, Roeder, et al., 2020). Some insect taxa are benefiting from rising temperatures, which can increase local populations (Baker et al., 2021) and range sizes (Termaat et al., 2019). However, as temperatures continue to rise and increase more rapidly, negative impacts on insect productivity are expected (Warren et al., 2018). This relationship is predicted by thermal performance theory, which hypothesizes that insect fitness, as measured by biomass or other performance indicators, will have a unimodal response to temperature (Kingsolver & Huey, 2008; Sinclair et al., 2016).

Responses of precipitation regimes to climate change vary with region, but forecasts generally suggest increased frequency of both heavy precipitation events and droughts (Myhre et al., 2019). High precipitation increases insect mortality and shortens the period of time insects are flying (Totland, 1994). Indirect effects of precipitation on flying insects mediated by plants

(e.g. altering plant phenology or plant nutrition) are context-dependent but increasing rainfall in average to wet climates is often detrimental (Lawson & Rands, 2019).

Changing land-cover due to human activities is additionally a major threat to insects (Wagner, 2020), causing loss of resources and nesting locations at local scales, to fragmented habitats at larger scales (Newbold et al., 2020). Heavily human-modified landscapes come with associated pressures, such as eutrophication and pesticide use with agricultural intensification (Carvalheiro et al., 2020; Goulson et al., 2018), and urban light pollution (Owens et al., 2020), reducing both insect diversity (Fenoglio et al., 2020; Piano et al., 2020), and biomass (Macgregor et al., 2019; Svenningsen et al., 2020).

Here we ask how climate and land-cover affect flying insect biomass across the growing season and 84 locations ranging over 7° latitude during the first year of monitoring (2019) of the German Malaise Trap Program. We hypothesize **(H1)** the effect of temperature on insect biomass will **a)** be unimodal, and **b)** decline at locations where local temperatures with the greatest increase above long-term averages. We hypothesize **(H2)** that flying insect biomass will decline with increasing precipitation due to reduced flying activity. Finally, we predict **(H3)** flying insect biomass will be lower in land-cover types with larger anthropogenic impacts such as urban and agricultural areas. We additionally conducted an exploratory analysis to see if the date of peak biomass varied with climate, land-cover type, or elevation and to examine if identified significant environmental drivers of insect biomass were the result of co-variation with biomass phenology (e.g. if positive predictors resulted in capturing a phenological interval with higher biomass). The broad spatial coverage allows us to examine drivers of flying insect biomass using a macroecological gradients approach (Peters et al., 2019; Pianka, 1966).

METHODS

German Malaise Trap Program

The German Malaise Trap Program currently comprises 31 German Long-Term Ecological Research (LTER-D) and National Natural Landscape sites (https://www.ufz.de/lter-d/index.php?de=46285). The program was established in early 2019 to investigate long-term trends in flying insect biomass and species composition using DNA metabarcoding. In each site, one to six locations were selected and one malaise trap was installed per location. All traps measured 1.16 m^2 on each side (Fig. S1). We examine here the 2019 biomass data retrieved from 25 of the 31 sites; the remaining sites began sampling in 2020 and are not analyzed in this study. To fill spatial gaps, we included 8 sites in Bavaria from an additional project using the same malaise trap type and measurement methods. Overall, this study includes 1039 samples from 84 locations and 33 participating sites distributed across Germany (Fig. 1; Table S1). Traps ran from early April to late October 2019 and were usually emptied every two weeks (14.03 days ± 0.06 SE; ranging 7-29 days). Some traps ran for shorter durations and several samples were lost due to animal or wind damage. By sampling across all times of day for the duration of the growing season, these data represent a wide variety of flying insect taxa across a large range of seasonal and diurnal flight periodicity.

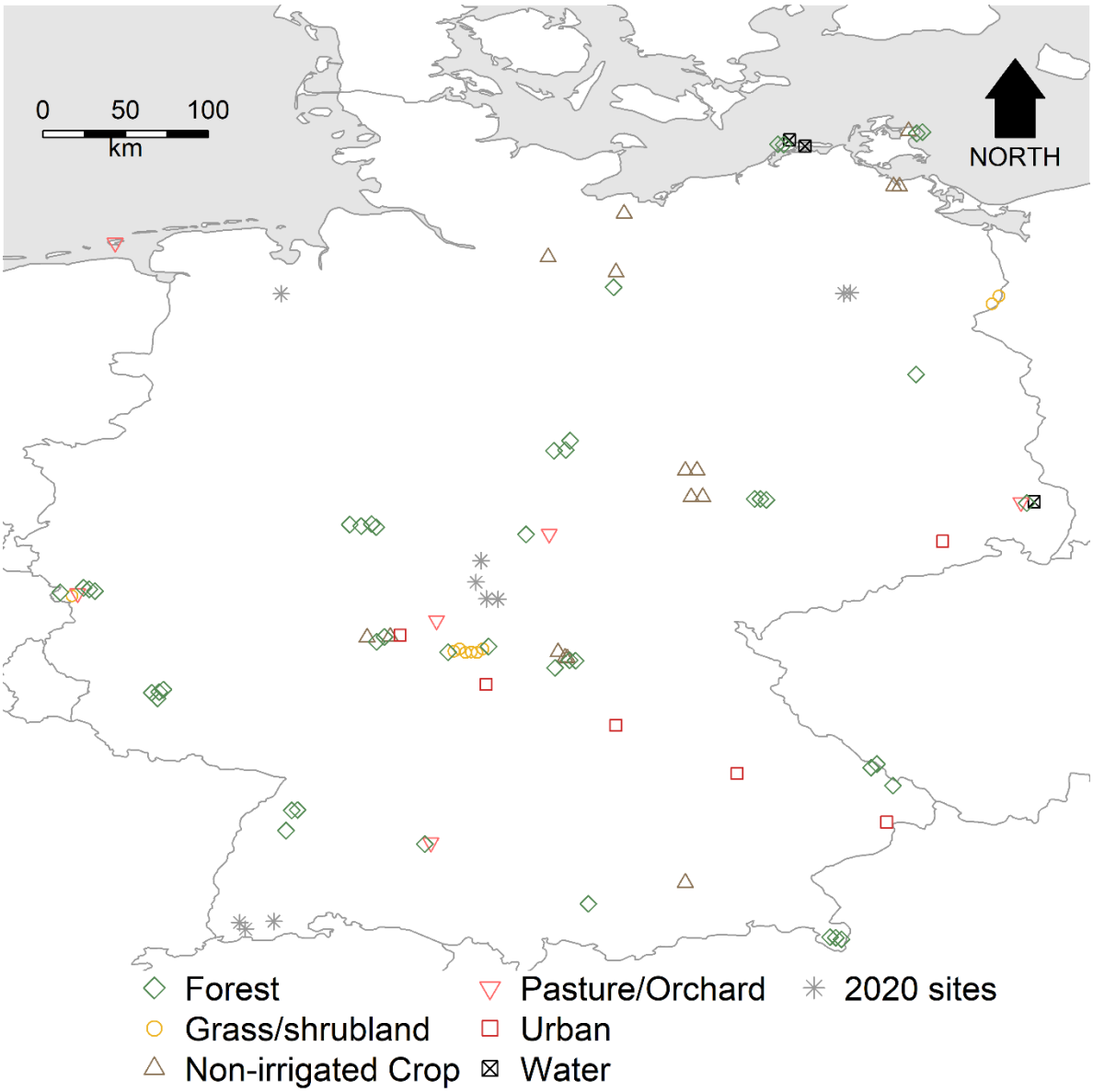

Figure 1. Malaise trap locations where samples were collected beginning in 2019 are identified by the dominant land-cover in the surrounding 1 km. Points coded as stars indicate trap locations at which sampling began in 2020 and are incorporated to show the full extent of the current program but are not included in the analyses. Overlapping locations were jittered longitudinally to improve visualization.

Lab procedures

Insect biomass was wet weighed to preserve samples for future identification. Alcohol was filtered in a stainless steel sieve (0.8 mm mesh width) following the procedure in Hallmann et al. (2017), with one modification: instead of waiting until alcohol drops occurred >10 seconds apart, samples were filtered for a standard five minutes prior to weighing to the nearest 0.01g.

Climate

Monthly means of maximum and minimum temperatures, and monthly cumulative precipitation (henceforth tmax, tmin, and precipitation) were extracted from each location from 2019 using the Terraclimate dataset (Abatzoglou et al., 2018), and from 1960-2018 using the CRU-TS 4.03 dataset (Harris et al., 2014) downscaled with WorldClim 2.1 (Fick & Hijmans, 2017). Data from both time periods (2019 and 1960-2018) were not available from either dataset alone. Both datasets have spatial resolutions of 2.5 arc minutes (~21 km^2) with our 84 trap locations occurring in 72 separate climate grid cells.

Tmax and tmin in 2019 were higher than 1960-2018 averages, especially during summer months (Fig. 2a) and were highly correlated ($R^2 = 0.97$). Therefore, we used only tmax in our analyses. Annual precipitation was slightly lower in 2019 (784 mm ± 32 SE) relative to the 1960-2018 average (842 mm ± 32 SE), with summer months comprising the driest period, but high variation existed across months (Fig. 2b). No latitudinal temperature gradient existed across our sampling locations in 2019 (Fig. S2a) or long-term averages (Fig. S2b), likely due to a negatively correlation between elevation and latitude (Fig. S3). However, southern latitudes in

2019 experienced temperatures exceeding long-term averages to a greater degree than northern latitudes (Fig. S2c) and had higher precipitation (Fig. S2d).

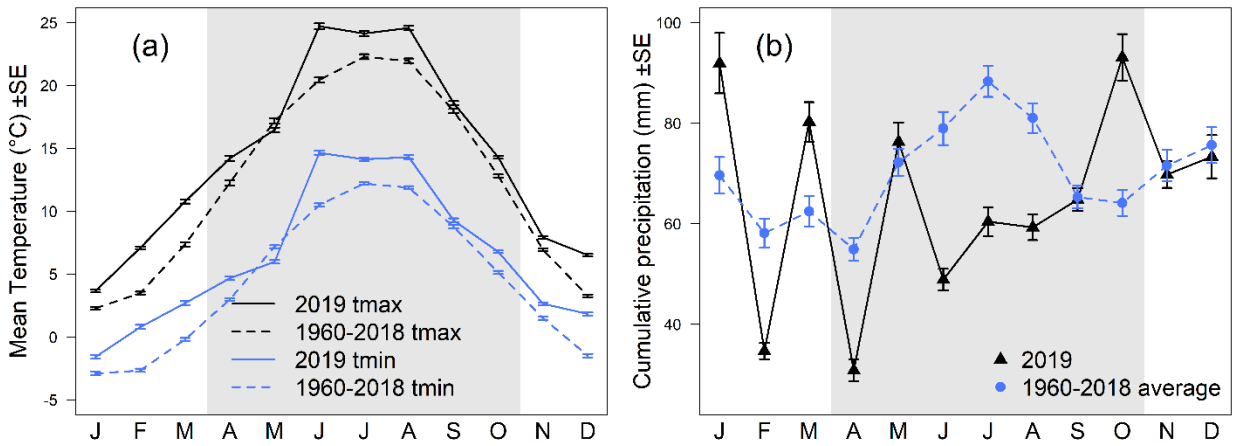

Figure 2. Comparison of climate at the 84 trap locations between 2019 and long-term average (1960-2018) including the average maximum monthly temperatures (tmax) and minimum monthly temperatures (tmin) in °C ± standard error (a) and cumulative monthly precipitation in mm ± standard error (b). Period of the year in which malaise trap sampling occurred is shaded in grey.

Land-cover

Land-cover categories in a 1-km buffer around each location were extracted using the 2018 CORINE dataset (European Union, Copernicus Land Monitoring Service, 2018). Previous work suggests that at scales larger than 1-km, insects have weaker responses to land-cover buffers (Seibold et al., 2019). The 30 CORINE land-cover types were pooled into eight categories: urban (7.5% of surrounding land-cover), intensive agriculture (2.3%), non-irrigated agriculture (15.9%), pasture/orchard (12.7%), forest (44.7%), grassland/shrubland (12.1%), freshwater (3.9%), and saltwater (0.9%).

Elevation

Elevation (m above sea level) was extracted using the Digital Terrain Model with 200-m grid widths (DGM200) from the German Federal Agency for Cartography and Geodesy (GeoBasis-DE / BKG, 2013). Elevation varied from 0 m on a barrier island in northeast Germany, to 1413 m in the German Alps.

All GIS data extraction was conducted in QGIS ver. 3.14 (QGIS.org, 2020).

Model selection

To identify drivers of insect biomass, we used an Akaike Information Criterion corrected for small sample sizes (AIC_c) framework (Burnham & Anderson, 2003); first building an *a priori* full model, comparing AIC_c of models with and without spatial autocorrelation to test for spatial non-independence, and then comparing all possible reduced models of fixed effects using the *dredge* function in the R package "MuMIn" (Bartoń, 2016). Mixed models were fit using the R package "lme4" (Bates et al., 2015). All analyses were conducted in R ver. 4.0.3 (R Core Team, 2020). To reduce variance inflation due to land-cover categories being percentages, we removed land-cover categories from the model starting with the least common until the variance inflation factor (VIF) was <10 (Montgomery et al., 2021); this removed the land-cover types of freshwater, intensive agriculture, and saltwater. VIF was calculated using the "car" package in program R (Fox & Weisberg, 2019). Initial analyses substituting the Land Use Index (LUI; Büttner, 2014) for land-cover percentages resulted in no top models containing LUI. We included the 2nd degree polynomial of the sampling period to capture the season pattern of

biomass. Sampling period refers to the half-month period most overlapping trap sampling days, and is numerical (e.g. first half of April = sampling period 1). Tmax and precipitation predictors correspond to the month in which the majority of sampling days occurred. Tmax was first included as a second order polynomial; however while all top models included the fixed effect of "poly(tmax,2)", the second order polynomial term of tmax was never significant; thus we replaced this parameter with a linear "tmax" term. We initially wished to include the 2019 temperatures minus the long-term average (Δ temp) as a driver, but this variable caused inflation with sampling period and thus was excluded. Precipitation and elevation were scaled by dividing by 100.

The full model contained the response variable of sample biomass in mg/day all 84 locations and was log10(x+1) transformed to correct for a log-skewed distribution. Fixed predictors of tmax, precipitation, elevation, % cover of the five most dominant land-cover categories, the 2nd degree polynomial of sampling period (poly(period,2)), and a random effect of trap location to account for repeated observations. We tested five models fitting spatial autocorrelation (exponential, Gaussian, linear, rational quadratic, and spherical correlation) and compared their AIC_c values with a model without a spatial correlation argument (Zuur et al., 2009). The model with the lowest AIC_c was the model without a spatial autocorrelation term; thus we proceeded with this model when selecting for fixed effects. Models with a $\Delta AIC_c < 2$ are considered parsimonious (Burnham & Anderson, 2003) and reported.

Temperature variation

We wished to further examine our hypothesis that the effects of temperature on flying insect biomass would decrease when local temperatures exceeded long-term averages, and examine how responses varied across sampling months. We were prohibited from including Δtemp (the deviation in monthly maximum temperatures from long-term averages) in the mixed model due to high variance inflation with sampling period. With the aim of reduce complexity due to variation in timing of sample collection across locations, and eliminate repeated sampling within a location/month, we calculated an average value of biomass (mg/day) per location and month by computing a monthly weighted average of insect biomass. Our calculation assumes traps caught the same amount of biomass each day within a sample and allocates sample biomass to each month weighed by the number of sampling days (e.g. for a trap run with 1 day in month A and 13 days in month B we assumed 1/14th of the biomass was collected in month A and 13/14^{ths} was in month B). With these assumptions, the average biomass B*ij* (mg/day) of location *i* in month *j* is a weighted average of the n samples occurring in the month according to the following formula:

Eq. 1

$$B_{i,j} = \frac{\sum_{k=1}^{n}(b_{ijk} \times D_{k,j} \div D_k)}{\sum_{k=1}^{n} D_{k,j}}$$

Where b_{ijk} = the total biomass (mg) at location *i* occurring at least partially in month *j* for a sample *k*, n= the total number of samples occurring at least partially in month *j* for location *i*, $D_{k,j}$ = the number of sampling days occurring in month *j* for a given sample *k*, D_k = the total number of sampling days for a given sample *k*

For each month (April- October), we then tested for an interaction between monthly tmax and Δ temp (2019 tmax minus the long-term average tmax) for the corresponding location/month

on log10 transformed $B_{i,j}$. We visualized the results using the R package "effects" (Fox & Weisberg, 2019).

Dominant land-cover categories

To visualize changes in flying insect biomass with land-cover, we plotted biomass/day over median day of sampling for locations corresponding to each dominant land-cover. Dominant land cover refers to the land cover type with the highest percentage in the 1 km buffer surrounding each location. The AIC_c analysis is our primary test of differences in biomass between land-cover types and uses land cover percentages rather than dominant land covers. However, we additionally used Welch's t-tests to identify significant differences between log10(x +1) transformed $B_{i,j}$ for all locations, and locations corresponding to each dominant land-cover within each month. No locations had surroundings dominated by intensive agriculture. Locations dominated by saltwater (n=1) and freshwater (n=2) were excluded due to low replication.

Peak biomass

To calculate the day of the year of peak biomass, we fit splines on the relationship between biomass (mg/day) of each sample and the median day of the year of each sample for each location using the "smooth.spline" function in program R. We then extracted the day of the year when the maximum value of the fitted spline occurred (see Fig. S4 for an example). We excluded locations where the maximum extracted value occurred at either end of the sampling interval, assuming these sampling locations may not have captured the peak biomass date; in total we

were able to calculate peak biomass date for 73 locations. We then followed the same AIC_c model selection procedure as was used for determining drivers of insect biomass to conduct model selection on drivers of peak biomass. The full *a priori* model was a linear regression which included the response variable of peak biomass date, and the response variables of the average monthly 2019 tmax from the beginning of the year (January) to the last main sampling month (October), the average Δtemp (2019 tmax minus long-term tmax) from January to October, the cumulative precipitation from January to October, elevation, and the % cover of the five most dominant land-cover categories. Precipitation and elevation were scaled by dividing by 100.

RESULTS

Mean flying insect biomass averaged 2,329 ± 79 SE mg/day and varied from >10 to 17,543 mg/day. Biomass increased from 734 ± 98 SE mg/day in early April, to a peak of 5,356 ± 401 SE mg/day in late June, declining to 568 ± 111 SE mg/day in late October. AIC_c model comparison selected two competing top models (Table S2) with both containing tmax, percent forest cover, and sampling period, then second model additionally containing elevation as predictors of flying insect biomass (Table 1). The top model explained 43-45% of the variance in flying insect biomass without location information (marginal R^2) and 73% of flying insect biomass was accounted for when including the random effect of location identity (conditional R^2; Table S2).

Table 1. Top AIC_c models. AIC_c model selection for predictors of flying insect biomass resulted in two top models (a & b). See Table S2 for AIC_c parameters. Both models include the

random variable of trap location. T-tests use Satterthwaite's method. Poly(period,1) and poly(period,2) indicate the first and second order terms of the 2nd degree polynomial for sampling period respectively. Other predictor variables include the percent forest in a surrounding 1 km buffer (%forest) and monthly maximum temperature (tmax). Model characteristics include estimate (Est), standard error (SE), degrees of freedom (df), t-value, and p-value (*P*).

	Est	**SE**	**df**	**t-value**	***P***
a.) Model 1					
Intercept	2.278	0.122	952	18.73	< 0.001
%forest	-0.319	0.109	82	-2.93	0.0043
poly(period,1)	-4.124	0.329	952	-12.52	< 0.001
poly(period,2)	-4.402	0.707	952	-6.23	< 0.001
tmax	0.047	0.005	952	9.53	< 0.001
b.) Model 2					
Intercept	2.211	0.123	952	18.04	< 0.001
elevation	0.036	0.013	81	2.72	0.008
%forest	-0.487	0.122	81	-4	< 0.001
poly(period,1)	-4.129	0.329	952	-12.54	< 0.001
poly(period,2)	-4.288	0.707	952	-6.07	< 0.001
tmax	0.048	0.005	952	9.69	< 0.001

Climate

Flying insect biomass increased with 2019 tmax (Table 1a, Fig. S5a), and declined with increasing elevation (Table 1b, Fig. S5b). There was a significant interaction between tmax and Δtemp in the mid-season sampling months of June and July. In these two months tmax had a positive effect on flying insect biomass at locations with low Δtemps, shifting to a negative effect of tmax on flying insect biomass at locations with high Δtemps (Fig. 3; Table S3). Significant interactions between tmax and Δtemps were not found in other sampling months (Fig. 3; Table

S3). The slope of the effect of temperature on flying insect biomass was steeper with lower Δ temperatures in April, August, and September, though not significantly. This pattern flipped in May and October where the slope of the effect of temperature on flying insect was steeper with higher Δ temperatures, likely due to colder temperatures in these months, though again the interaction was not significant (Fig. 3; Table S3).

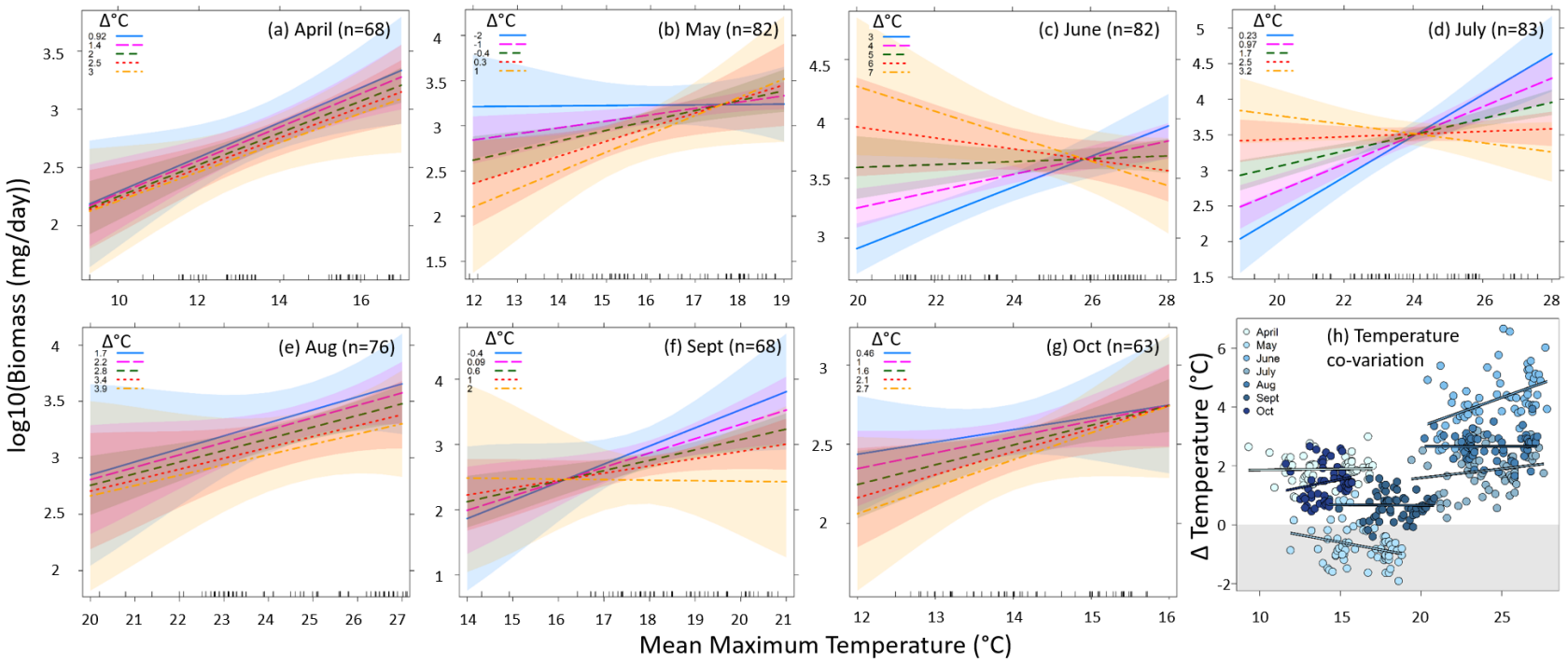

Figure 3. The effect of temperature on flying insect biomass was positive at the beginning of the growing season in (a) April, and (b) May regardless of Δtemp (2019 tmax minus the long-term average tmax), shifted from positive to negative with increasing Δtemp in (c) June and (d) July, and again became more positive with temperature independent of Δtemp in (e) August, (f) September, and (g) October. Number of locations with sampling (n) within each month are provided within panels a-g. While hotter months tended to have higher Δtemps, there was no consistent relationship between tmax and Δtemps within months (h). Significant interactions between tmax and Δtemp occurred in June and July; all model coefficients are provided in Table S3

Land-cover

Flying insect biomass declined with % forest in the 1 km buffer surrounding each trap location (Table 1). No other land cover categories appeared as drivers of insect biomass. Categorizing locations by dominant land-cover suggested grassland/shrublands had the highest biomass in the mid growing season (June/July; Fig. 4c), while non-irrigated cropland supported above-average biomass at either end of the growing season (May and September; Fig. 4e). Higher biomass in urban-dominated locations (April and July-September; Fig. 4f) may be due to urban-dominated locations being in southern Germany (Fig. 1) which tended to be slightly warmer (Fig. S2).

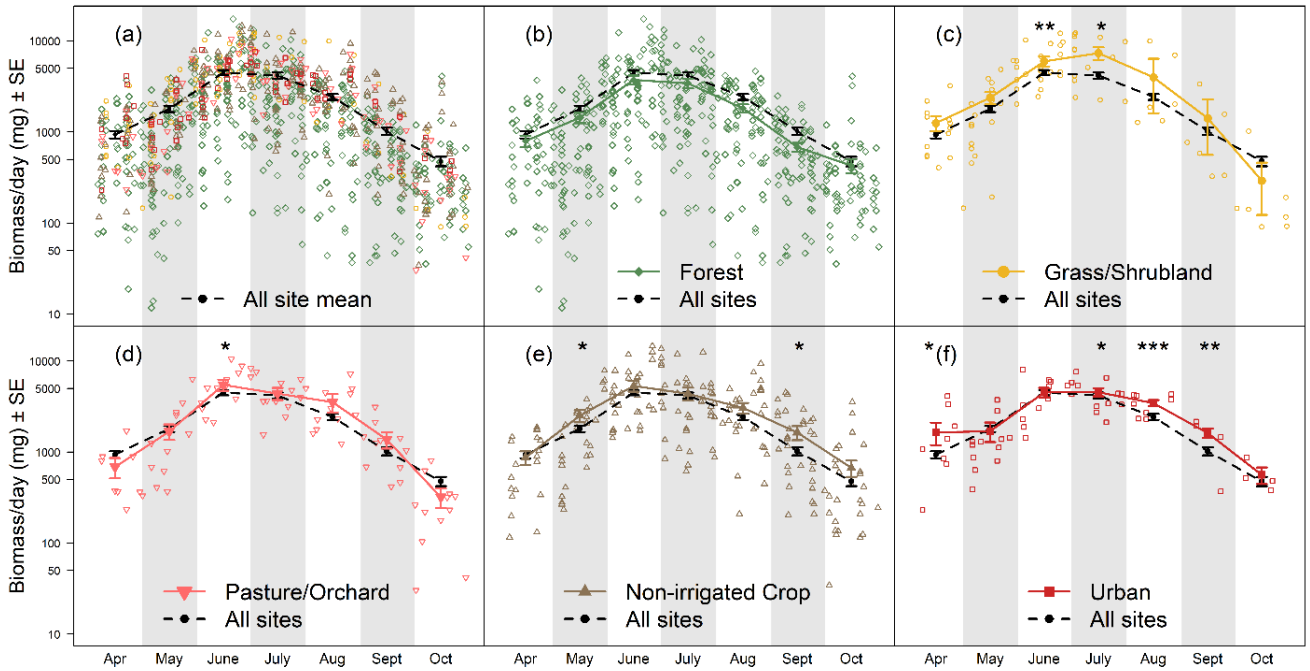

Figure 4. Biomass over the median sampling day across all 84 trap locations (a), and comparisons between all locations and locations with surroundings dominated by forests (b; n=44), grassland/shrubland (c; n=9), pasture/orchard (d; n=6), non-irrigated cropland (e; n=16), and urban environments (f; n=6). Point shapes and colors in panel (d) match the dominant land category following shapes and colors in panels b-f. Mean and standard error are provided for biomass within each land cover category and month. Stars indicate significant differences within each month between dominant land cover categories and all-location averages (* = 0.05 > P > 0.01, ** = 0.01 > P > 0.001, *** = P < 0.001).

Peak biomass

The day of the year of peak biomass varied from 148.5 (May 28-29th) to 219 (Aug. 7th) across the 73 trap locations from which it was estimable (averaging 175.1 [June 24th] ± 1.6 days SE). Model selection resulted in 12 top models with $\Delta AIC_c < 2$ (Table S4). The most consistent result was earlier peak biomass dates in locations with more surrounding grassland/shrubland. Other drivers of peak biomass date included earlier peak biomass date with increasing elevation, Δtemp, and % forest, and later peak biomass date with increasing precipitation, % pasture/orchard, and % urban surroundings. However, predictive power of top models of peak insect biomass date was low (R^2 s ranging from 0.07-0.14; Table S4).

DISCUSSION

In a study of 84 locations widely distributed across Germany, we found strong effects of temperature on flying insect biomass. Biomass increased linearly with temperature in contrast to the unimodal relationship predicted by the first prediction of our first hypothesis (**H1a**); however, when high, positive deviations from long-term average temperatures were combined with the hotter summer months of June and July, temperature no longer had a positive effect on flying insect biomass, in support of our second hypothesis (**H1b)**. Temperatures in June 2019 were especially hotter than long-term averages across trap locations (averaging 4.3°C ± 0.1 SE). In contrast, insect biomass only increased with temperature in May 2019, which was cold relative to the long-term averages (averaging -0.7°C ± 0.1 SE). The negative effect of high deviations from long-term temperature averages suggests insects are adapted to local temperature

conditions. Rapid rises in temperature may exceed locally established tolerance limits, having negative effects on insect communities even in colder climate regions.

A decelerating benefit of temperature in locations with greater increases in temperature is consistent with previous long-term studies of insects. In a study of two surveys of ant communities across North America conducted 20 years apart, and finding that sites with the largest increases in temperature had the largest declines in colony density (Kaspari et al., 2019). Hallmann et al. (2017) found a positive effect of temperature on insect biomass; however, biomass loss over time was greatest in mid-summer, when temperatures are highest. Flying insects may be more affected by rising temperatures than non-flying insects as they cannot buffer high temperatures by burrowing in soil or plant tissue (Baudier et al., 2015; Wagner, 2020). We predict future monitoring will detect increasingly negative effects of temperature due to ongoing climate warming, as temperature begins to exceed species' optimum temperature ranges.

Climate change predictions for Germany suggest slight increases in cumulative annual precipitation, but shifts in the timing of rainfall and drier summers (Bender et al., 2017). The 2019 growing season matched this prediction with June, July and August being much drier than the long-term average and with the wettest month of the study period being October. As insects can detect changes in barometric pressure and will stop flying if they sense storms approaching (Pellegrino et al., 2013), we predicted increased rainfall would result in reduced flight activity, reducing insect biomass. However, precipitation was not a significant predictor of flying insect biomass as predicted by **H2** potentially due to low variation in precipitation across locations.

With ~75% of global land significantly altered by human activities (IPBES, 2019), land-cover change and land use intensification is a major contributor to insect decline (Díaz et al., 2019; Potts et al., 2010; Winfree et al., 2011). In contrast to **H3,** we did not detect negative

effects of urban and agricultural land-cover on flying insect biomass. The strongest effect of surrounding land-cover was reduced insect biomass in forests. Forests may provide fewer floral resources than open fields (Jachuła et al., 2017). Alternatively, forest vegetation structure may limit insect movement through the landscape, reducing trap catch in comparison to open systems like grasslands (Cranmer et al., 2012). The absence of an effect of heavily human-impacted habitats on flying insect biomass may be due to a minority of our locations surrounded by high proportions of these land-cover types, especially intensive agriculture. Higher temperatures in urban areas may explain the above average biomass in spring and late summer/autumn, while also making insects in urban areas more vulnerable to future warming in mid-summer. Additionally, large variability exists in insect habitat quality of urban areas and agricultural land, ranging from paved expanses and areas with intensive pesticide use to urban gardens and low intensity organic farms (Bengtsson et al., 2005; Hausmann et al., 2020). While moderately impacted by human activity, non-irrigated agricultural areas, pasture land, and orchards in this study tended to support higher biomass, suggesting these land use types may provide suitable habitats for Germany's flying insects. Alternatively, fertilization and the prevalence of monoculture on conventional farms may increase insect biomass through alleviating nutrient limitation and providing high concentrations of host plants, while not benefiting insect biodiversity (Haddad et al., 2000; Root, 1973).

While the date of peak biomass ranged from late May to early August across trap locations and varied with land-cover types, the percent variance explained by environmental drivers was low. The average temperature at trap locations was not a predictor of the date of peak biomass, suggesting the overall positive response of flying insect biomass was not driven by shifts in biomass phenology. However, top models included a weak effect of locations with

higher Δ temperatures having earlier peak biomass dates. Land-cover types and temperature may also interact in their effects on flying insect biomass, though our number of trap locations is prohibitory of examining many interaction terms. Earlier peak biomass dates in grasslands and forests compared to urban areas and pasture/orchard is indicative of differences between more natural and more human-modified areas and supported by previous work finding later phenologies of butterflies (Diamond et al., 2014) and flower bloom times (Li et al., 2021) in urban areas.

Comparison with Hallmann et al. 2017

A recent study (Hallmann et al., 2017) reported large declines in flying insect biomass from 63 German locations over 27 years. However, sampling locations greatly varied with years and the majority (58 out of 63) were clustered in central-west Germany; the sites do not have representative coverage of Germany or comprise an extensive latitudinal gradient (coverage of 2° latitude). Average insect biomass reported in Hallmann et al. (2017) varied from 9,192 mg/day in 1989 to 2,531 mg/day in 2016 (May-Sept average; no April 1989 sampling was conducted). In comparison, our traps collected a monthly average of 2,404 mg/day in May-Sept. However, Hallmann et al. (2017) used traps which were ~51% larger (1.79 m^2 per side) than those in this study (1.16 m^2), suggesting higher trap catch in this study relative to the last sampling year (2016) in Hallmann et al. (2017), if trap size has an appreciable positive effect on catch. This discrepancy is most likely due to differences in sampling locations as our study cover a wider range of locations and habitats than examined in Hallmann et al. (2017), but we cannot rule out an increase in biomass of flying insects in Germany.

Caveats

Insect biomass is a common currency ecosystem-level measure of insect productivity and is an index of energy availability for higher trophic levels. Nonetheless, from biomass alone we cannot differentiate variation in abundance, body size, species diversity, or dominance. High temperatures may reduce insect body sizes within species (Atkinson, 1994; Klockmann et al., 2017; Polidori et al., 2020) or favor smaller species (Bergmann, 1848; Daufresne et al., 2009; Merckx et al., 2018). While one long-term study of flying insects in the Netherlands found no evidence of higher rates of decline in larger species over the past two decades (Hallmann et al., 2020), larger-bodied species may have become rare earlier in the last century (Seibold et al., 2015). Climate and land-cover change may otherwise alter insect communities by favoring particular trophic levels (Welti, Kuczynski, et al., 2020), invasive (Ju et al., 2017), or pest species (Bernal & Medina, 2018). The lack of an overall unimodal relationship temperature may be a result of the coarse taxonomic (flying insects) and temporal (~2 week) sample resolution in comparison to other studies (e.g. Kühsel & Blüthgen, 2015). Additionally, malaise traps do not collect all flying insects with larger insects like butterflies often being underrepresented. Finally, this monitoring program does not yet include multi-year coverage of flying insect trends. However, such space for time, or ecological gradients approaches have a long and fruitful history in ecology and are a useful method for providing predictions of temporal trends in the absence of time series (Peters et al., 2019; Pianka, 1966).

Future directions: Importance of large-scale insect monitoring programs

In this first study of flying insect biomass from the German Malaise Trap Program, we find that even in a temperate climate, the positive effect of temperature on flying insect biomass diminished when combined with high positive deviations in temperature from the long-term average, and hotter mid-summer months. These interactions could not have been elucidated without growing season-long monitoring across a large number of locations and a thermal gradient. Large-scale, long-term standardized monitoring is a critical tool to disentangle potential drivers of insect decline and understand how this varies with region and taxa. Empirical studies of insect communities often lack the spatial coverage to be broadly representative across habitats (but see Jeliazkov et al., 2016; Wepprich et al., 2019). Meta-analyses have large spatial coverage, but must reckon with variable research goals and methodologies (Gurevitch & Mengersen, 2010). Spatially distributed monitoring efforts of ecological communities primarily target plants and vertebrates but not insects (Eggleton, 2020). Notable exceptions include mosquito and ground beetle monitoring by the US National Ecological Observation Network (Thorpe et al., 2016), and several regional-scale Lepidoptera monitoring programs (e.g. Dennis et al., 2019; Kühn et al., 2008; van Swaay et al., 2019). The Global Malaise Trap Program, operating since 2012 (http://biodiversitygenomics.net/projects/gmp/), and the Swedish Malaise Trap Program (operational from 2003-2006; Karlsson et al., 2020) are taxonomic treasure troves, though neither measure biomass. The German Malaise Trap Program helps to fill the gap of a distributed, standardized, and continuous monitoring program of flying insects for Germany. Malaise traps are currently being considered as a standard component of European insect biodiversity surveys, and this program provides a blueprint for a coordinated large-scale malaise trap sampling network (Haase et al., 2018). As highlighted by the recent insect decline debate

(Wagner et al., 2021), comprehensive and standardized monitoring is critical to meet the challenge of unravelling insect trends and drivers in the Anthropocene.

Acknowledgements

We thank Beatrice Kulawig, Monika Baumeister, Michael Ehrhardt, Sebastian Flinkerbusch, Michael Hinz, Reinhard Hölzel, Enno Klipp, Sebastian Keller, Linus Krämer, Gudrun Krimmer, Paula Kirschner, Beate Krischke, Johannes Lindner, Susanne Schiele, Verena Schmidt, Dragan Petrovic, Simon Potthast, Almuth Puschmann, Lena Unterbauer, Jan Weber, Roland Wollgarten, and the Auwaldstation Leipzig for assistance in the field and lab. We are grateful to the eLTER PLUS project (Grand Agreement No. 871128) for financial support to EARW and PH. This work was further supported by DFG AY12/6-4 to MA, DFG WE3081/21-4 to WWW, DFG MO2142/1-1 to MTM, and the Bavarian State Ministry of Science and the Arts.

REFERENCES

Abatzoglou, J. T., Dobrowski, S. Z., Parks, S. A., & Hegewisch, K. C. (2018). TerraClimate, a high-resolution global dataset of monthly climate and climatic water balance from 1958–2015. *Scientific Data*, *5*(1), 170191. https://doi.org/10.1038/sdata.2017.191

Atkinson, D. (1994). Temperature and organism size—A biological law for ectotherms? In M. Begon & A. H. Fitter (Eds.), *Advances in Ecological Research* (Vol. 25, pp. 1–58). Academic Press. https://doi.org/10.1016/S0065-2504(08)60212-3

Baker, N. J., Jourdan, J., Pilotto, F., & Haase, P. (2021). Drivers of long-term changes in aquatic macroinvertebrate communities within a near pristine mountainous stream. *Science of The Total Environment*, *785*, 14685.

Barnes, A. D., Weigelt, P., Jochum, M., Ott, D., Hodapp, D., Haneda, N. F., & Brose, U. (2016). Species richness and biomass explain spatial turnover in ecosystem functioning across tropical and temperate ecosystems. *Philosophical Transactions of the Royal Society B: Biological Sciences*, *371*(1694), 20150279. https://doi.org/10.1098/rstb.2015.0279

Bartoń, K. (2016). *MuMIn: Multi-Model Inference* (1.43.6) [Computer software]. https://CRAN.R-project.org/package=MuMIn

Bates, D., Mächler, M., Bolker, B., & Walker, S. (2015). Fitting linear mixed-effects models using lme4. *Journal of Statistical Software*, *67*(1), 1–48. https://doi.org/10.18637/jss.v067.i01

Baudier, K. M., Mudd, A. E., Erickson, S. C., & O'Donnell, S. (2015). Microhabitat and body size effects on heat tolerance: Implications for responses to climate change (army ants: Formicidae, Ecitoninae). *The Journal of Animal Ecology*, *84*(5), 1322–1330. https://doi.org/10.1111/1365-2656.12388

Bender, S., Butts, M., Hagemann, S., Smith, M., Vereecken, H., & Wendland, F. (2017). *Einfluss des Klimawandels auf die terrestrischen Wassersysteme in Deutschland. Eine Analyse ausgesuchter Studien der Jahre 2009 bis 2013* (No. 29). Climate Service Center.

Bengtsson, J., Ahnström, J., & Weibull, A.-C. (2005). The effects of organic agriculture on biodiversity and abundance: A meta-analysis. *Journal of Applied Ecology*, *42*(2), 261–269. https://doi.org/10.1111/j.1365-2664.2005.01005.x

Bergmann, C. (1848). *Über die Verhältnisse der Wärmeökonomie der Thiere zu ihrer Größe*. http://archive.org/details/bub_gb_EHo-AAAAcAAJ

Bernal, J. S., & Medina, R. F. (2018). Agriculture sows pests: How crop domestication, host shifts, and agricultural intensification can create insect pests from herbivores. *Current Opinion in Insect Science*, *26*, 76–81. https://doi.org/10.1016/j.cois.2018.01.008

Burnham, K. P., & Anderson, D. R. (2003). *Model selection and multimodel inference: A practical information-theoretic approach* (2nd ed.). Springer-Verlag. https://www.springer.com/gp/book/9780387953649

Büttner, G. (2014). CORINE land cover and land cover change products. In I. Manakos & M. Braun (Eds.), *Land Use and Land Cover Mapping in Europe: Practices & Trends* (pp. 55–74). Springer Netherlands. https://doi.org/10.1007/978-94-007-7969-3_5

Carvalheiro, L. G., Biesmeijer, J. C., Franzén, M., Aguirre-Gutiérrez, J., Garibaldi, L. A., Helm, A., Michez, D., Pöyry, J., Reemer, M., Schweiger, O., Den, B. L. van, WallisDeVries, M. F., & Kunin, W. E. (2020). Soil eutrophication shaped the composition of pollinator assemblages during the past century. *Ecography*, *43*(2), 209–221. https://doi.org/10.1111/ecog.04656

Cranmer, L., McCollin, D., & Ollerton, J. (2012). Landscape structure influences pollinator movements and directly affects plant reproductive success. *Oikos*, *121*, 562–568. https://doi.org/10.1111/j.1600-0706.2011.19704.x

Dangles, O., Crespo-Pérez, V., Andino, P., Espinosa, R., Calvez, R., & Jacobsen, D. (2011). Predicting richness effects on ecosystem function in natural communities: Insights from high-elevation streams. *Ecology*, *92*(3), 733–743. https://doi.org/10.1890/10-0329.1

Daufresne, M., Lengfellner, K., & Sommer, U. (2009). Global warming benefits the small in aquatic ecosystems. *Proceedings of the National Academy of Sciences*, *106*(31), 12788–12793. https://doi.org/10.1073/pnas.0902080106

Dennis, E. B., Brereton, T. M., Morgan, B. J. T., Fox, R., Shortall, C. R., Prescott, T., & Foster, S. (2019). Trends and indicators for quantifying moth abundance and occupancy in Scotland. *Journal of Insect Conservation*, *23*(2), 369–380. https://doi.org/10.1007/s10841-019-00135-z

Diamond, S. E., Cayton, H., Wepprich, T., Jenkins, C. N., Dunn, R. R., Haddad, N. M., & Ries, L. (2014). Unexpected phenological responses of butterflies to the interaction of urbanization and geographic temperature. *Ecology*, *95*(9), 2613–2621. https://doi.org/10.1890/13-1848.1

Díaz, S., Settele, J., Brondízio, E. S., Ngo, H. T., Agard, J., Arneth, A., Balvanera, P., Brauman, K. A., Butchart, S. H. M., Chan, K. M. A., Garibaldi, L. A., Ichii, K., Liu, J., Subramanian, S. M., Midgley, G. F., Miloslavich, P., Molnár, Z., Obura, D., Pfaff, A., … Zayas, C. N. (2019).

Pervasive human-driven decline of life on Earth points to the need for transformative change. *Science*, *366*(6471). https://doi.org/10.1126/science.aax3100

Didham, R. K., Basset, Y., Collins, C. M., Leather, S. R., Littlewood, N. A., Menz, M. H. M., Müller, J., Packer, L., Saunders, M. E., Schönrogge, K., Stewart, A. J. A., Yanoviak, S. P., & Hassall, C. (2020). Interpreting insect declines: Seven challenges and a way forward. *Insect Conservation and Diversity*, *13*(2), 103–114. https://doi.org/10.1111/icad.12408

Eggleton, P. (2020). The state of the world's insects. *Annual Review of Environment and Resources*, *45*(1), 61–82. https://doi.org/10.1146/annurev-environ-012420-050035

European Union, Copernicus Land Monitoring Service. (2018). *European Environment Agency (EEA)*.

Fenoglio, M. S., Rossetti, M. R., & Videla, M. (2020). Negative effects of urbanization on terrestrial arthropod communities: A meta-analysis. *Global Ecology and Biogeography*, *29*(8), 1412–1429. https://doi.org/10.1111/geb.13107

Fick, S. E., & Hijmans, R. J. (2017). WorldClim 2: New 1-km spatial resolution climate surfaces for global land areas. *International Journal of Climatology*, *37*(12), 4302–4315. https://doi.org/10.1002/joc.5086

Fox, J., & Weisberg, S. (2019). *An R Companion to Applied Regression* (3rd Edition). Sage Publications, Inc.

GeoBasis-DE / BKG. (2013). *Digital Terrain Model grid wisth 200 m (DGM200)*. Bundesamt für Kartographie und Geodäsie. http://www.bkg.bund.de

Goulson, D., Thompson, J., & Croombs, A. (2018). Rapid rise in toxic load for bees revealed by analysis of pesticide use in Great Britain. *PeerJ*, *6*, e5255. https://doi.org/10.7717/peerj.5255

Gurevitch, J., & Mengersen, K. (2010). A statistical view of synthesizing patterns of species richness along productivity gradients: Devils, forests, and trees. *Ecology*, *91*(9), 2553–2560. https://doi.org/10.1890/09-1039.1

Haase, P., Tonkin, J. D., Stoll, S., Burkhard, B., Frenzel, M., Geijzendorffer, I. R., Häuser, C., Klotz, S., Kühn, I., McDowell, W. H., Mirtl, M., Müller, F., Musche, M., Penner, J., Zacharias, S., &

Schmeller, D. S. (2018). The next generation of site-based long-term ecological monitoring: Linking essential biodiversity variables and ecosystem integrity. *Science of The Total Environment*, *613–614*, 1376–1384. https://doi.org/10.1016/j.scitotenv.2017.08.111

Habel, J. C., Samways, M. J., & Schmitt, T. (2019). Mitigating the precipitous decline of terrestrial European insects: Requirements for a new strategy. *Biodiversity and Conservation*, *28*(6), 1343–1360. https://doi.org/10.1007/s10531-019-01741-8

Haddad, N. M., Haarstad, J., & Tilman, D. (2000). The effects of long-term nitrogen loading on grassland insect communities. *Oecologia*, *124*(1), 73–84. https://doi.org/10.1007/s004420050026

Hallmann, C. A., Sorg, M., Jongejans, E., Siepel, H., Hofland, N., Schwan, H., Stenmans, W., Mueller, A., Sumser, H., Hoerren, T., Goulson, D., & de Kroon, H. (2017). More than 75 percent decline over 27 years in total flying insect biomass in protected areas. *Plos One*, *12*(10), e0185809. https://doi.org/10.1371/journal.pone.0185809

Hallmann, C. A., Zeegers, T., Klink, R. van, Vermeulen, R., Wielink, P. van, Spijkers, H., Deijk, J. van, Steenis, W. van, & Jongejans, E. (2020). Declining abundance of beetles, moths and caddisflies in the Netherlands. *Insect Conservation and Diversity*, *13*(2), 127–139. https://doi.org/10.1111/icad.12377

Harris, I., Jones, P. D., Osborn, T. J., & Lister, D. H. (2014). Updated high-resolution grids of monthly climatic observations—The CRU TS3.10 Dataset. *International Journal of Climatology*, *34*(3), 623–642. https://doi.org/10.1002/joc.3711

Hausmann, A., Segerer, A. H., Greifenstein, T., Knubben, J., Morinière, J., Bozicevic, V., Doczkal, D., Günter, A., Ulrich, W., & Habel, J. C. (2020). Toward a standardized quantitative and qualitative insect monitoring scheme. *Ecology and Evolution*, *10*(9), 4009–4020. https://doi.org/10.1002/ece3.6166

IPBES. (2019). *Summary for policymakers of the global assessment report on biodiversity and ecosystem services. S. Díaz, J. Settele, E. S. Brondízio E.S., H. T. Ngo, M. Guèze, J. Agard, A. Arneth, P. Balvanera, K. A. Brauman, S. H. M. Butchart, K. M. A. Chan, L. A. Garibaldi, K. Ichii, J. Liu, S.*

M. Subramanian, G. F. Midgley, P. Miloslavich, Z. Molnár, D. Obura, A. Pfaff, S. Polasky, A. Purvis, J. Razzaque, B. Reyers, R. Roy Chowdhury, Y. J. Shin, I. J. Visseren-Hamakers, K. J. Willis, and C. N. Zayas (eds.) (summary for policy makers, p. 11). IPBES secretariat. https://doi.org/10.5281/ZENODO.3553579

Jachuła, J., Denisow, B., & Wrzesień, M. (2017). Validation of floral food resources for pollinators in agricultural landscape in SE Poland: Validation of floral food resources for pollinators. *Journal of the Science of Food and Agriculture*, *98*. https://doi.org/10.1002/jsfa.8761

Janzen, D. H., & Hallwachs, W. (2019). Perspective: Where might be many tropical insects? *Biological Conservation*, *233*, 102–108. https://doi.org/10.1016/j.biocon.2019.02.030

Jeliazkov, A., Bas, Y., Kerbiriou, C., Julien, J.-F., Penone, C., & Le Viol, I. (2016). Large-scale semi-automated acoustic monitoring allows to detect temporal decline of bush-crickets. *Global Ecology and Conservation*, *6*, 208–218. https://doi.org/10.1016/j.gecco.2016.02.008

Ju, R.-T., Gao, L., Wei, S.-J., & Li, B. (2017). Spring warming increases the abundance of an invasive specialist insect: Links to phenology and life history. *Scientific Reports*, *7*(1), 14805. https://doi.org/10.1038/s41598-017-14989-3

Karlsson, D., Forshage, M., Holston, K., & Ronquist, F. (2020). The data of the Swedish Malaise Trap Project, a countrywide inventory of Sweden's insect fauna. *Biodiversity Data Journal*, *8*, e56286. https://doi.org/10.3897/BDJ.8.e56286

Kaspari, M., Bujan, J., Roeder, K. A., Beurs, K. de, & Weiser, M. D. (2019). Species energy and Thermal Performance Theory predict 20-yr changes in ant community abundance and richness. *Ecology*, *100*(12), e02888. https://doi.org/10.1002/ecy.2888

Kingsolver, J., & Huey, R. (2008). Size, temperature, and fitness: Three rules. *Evolutionary Ecology Research*, *10*, 251–268.

Klockmann, M., Kleinschmidt, F., & Fischer, K. (2017). Carried over: Heat stress in the egg stage reduces subsequent performance in a butterfly. *PLOS ONE*, *12*(7), e0180968. https://doi.org/10.1371/journal.pone.0180968

Kühn, E., Feldmann, R., Harpke, A., Hirneisen, N., Musche, M., Leopold, P., & Settelea, J. (2008). Getting the public involved in butterfly conservation: Lessons learned from a new monitoring scheme in Germany. *Israel Journal of Ecology and Evolution*, *54*(1), 89–103. https://doi.org/10.1560/IJEE.54.1.89

Kühsel, S., & Blüthgen, N. (2015). High diversity stabilizes the thermal resilience of pollinator communities in intensively managed grasslands. *Nature Communications*, *6*(1), 7989. https://doi.org/10.1038/ncomms8989

Lawson, D. A., & Rands, S. A. (2019). The effects of rainfall on plant–pollinator interactions. *Arthropod-Plant Interactions*, *13*(4), 561–569. https://doi.org/10.1007/s11829-019-09686-z

Li, D., Barve, N., Brenskelle, L., Earl, K., Barve, V., Belitz, M. W., Doby, J., Hantak, M. M., Oswald, J. A., Stucky, B. J., Walters, M., & Guralnick, R. P. (2021). Climate, urbanization, and species traits interactively drive flowering duration. *Global Change Biology*, *27*(4), 892–903. https://doi.org/10.1111/gcb.15461

Losey, J. E., & Vaughan, M. (2006). The economic value of ecological services provided by insects. *BioScience*, *56*(4), 311–323. https://doi.org/10.1641/0006-3568(2006)56[311:TEVOES]2.0.CO;2

Macgregor, C. J., Williams, J., Bell, J., & Thomas, C. (2019). Moth biomass increases and decreases over 50 years in Britain. *Nature Ecology and Evolution*. http://eprints.whiterose.ac.uk/151824/

Merckx, T., Souffreau, C., Kaiser, A., Baardsen, L. F., Backeljau, T., Bonte, D., Brans, K. I., Cours, M., Dahirel, M., Debortoli, N., De Wolf, K., Engelen, J. M. T., Fontaneto, D., Gianuca, A. T., Govaert, L., Hendrickx, F., Higuti, J., Lens, L., Martens, K., … Van Dyck, H. (2018). Body-size shifts in aquatic and terrestrial urban communities. *Nature*, *558*(7708), 113–116. https://doi.org/10.1038/s41586-018-0140-0

Montgomery, D. C., Peck, E. A., & Vining, G. G. (2021). *Introduction to linear regression analysis* (Vol. 6th). John Wiley & Sons.

Myhre, G., Alterskjær, K., Stjern, C. W., Hodnebrog, Ø., Marelle, L., Samset, B. H., Sillmann, J., Schaller, N., Fischer, E., Schulz, M., & Stohl, A. (2019). Frequency of extreme precipitation

increases extensively with event rareness under global warming. *Scientific Reports*, *9*(1), 16063. https://doi.org/10.1038/s41598-019-52277-4

Newbold, T., Bentley, L. F., Hill, S. L. L., Edgar, M. J., Horton, M., Su, G., Şekercioğlu, Ç. H., Collen, B., & Purvis, A. (2020). Global effects of land use on biodiversity differ among functional groups. *Functional Ecology*, *34*(3), 684–693. https://doi.org/10.1111/1365-2435.13500

Owens, A. C. S., Cochard, P., Durrant, J., Farnworth, B., Perkin, E. K., & Seymoure, B. (2020). Light pollution is a driver of insect declines. *Biological Conservation*, *241*, 108259. https://doi.org/10.1016/j.biocon.2019.108259

Pellegrino, A., Peñaflor, M. F., Nardi, C., Bezner-Kerr, W., Guglielmo, C., Bento, J. M., & Mcneil, J. (2013). Weather forecasting by insects: Modified sexual behaviour in response to atmospheric pressure changes. *PloS One*, *8*, e75004. https://doi.org/10.1371/journal.pone.0075004

Peters, M. K., Hemp, A., Appelhans, T., Becker, J. N., Behler, C., Classen, A., Detsch, F., Ensslin, A., Ferger, S. W., Frederiksen, S. B., Gebert, F., Gerschlauer, F., Gütlein, A., Helbig-Bonitz, M., Hemp, C., Kindeketa, W. J., Kühnel, A., Mayr, A. V., Mwangomo, E., … Steffan-Dewenter, I. (2019). Climate–land-use interactions shape tropical mountain biodiversity and ecosystem functions. *Nature*, *568*(7750), 88–92. https://doi.org/10.1038/s41586-019-1048-z

Pianka, E. R. (1966). Latitudinal gradients in species diversity: A review of concepts. *The American Naturalist*, *100*(910), 33–46.

Piano, E., Souffreau, C., Merckx, T., Baardsen, L. F., Backeljau, T., Bonte, D., Brans, K. I., Cours, M., Dahirel, M., Debortoli, N., Decaestecker, E., De Wolf, K., Engelen, J. M. T., Fontaneto, D., Gianuca, A. T., Govaert, L., Hanashiro, F. T. T., Higuti, J., Lens, L., … Hendrickx, F. (2020). Urbanization drives cross-taxon declines in abundance and diversity at multiple spatial scales. *Global Change Biology*, *26*(3), 1196–1211. https://doi.org/10.1111/gcb.14934

Polidori, C., Gutiérrez-Cánovas, C., Sánchez, E., Tormos, J., Castro, L., & Sánchez-Fernández, D. (2020). Climate change-driven body size shrinking in a social wasp. *Ecological Entomology*, *45*(1), 130–141. https://doi.org/10.1111/een.12781

Potts, S. G., Biesmeijer, J. C., Kremen, C., Neumann, P., Schweiger, O., & Kunin, W. E. (2010). Global pollinator declines: Trends, impacts and drivers. *Trends in Ecology & Evolution*, *25*(6), 345–353. https://doi.org/10.1016/j.tree.2010.01.007

QGIS.org. (2020). *QGIS Geographic Information System. Open Source Geospatial Foundation Project*.

R Core Team. (2020). *R: A language and environment for statistical computing* (4.0.3) [Computer software]. R Foundation for Statistical Computing. http://www.R-project.org/

Root, R. B. (1973). Organization of a plant-arthropod association in simple and diverse habitats: The fauna of collards (Brassica oleracea). *Ecological Monographs*, *43*(1), 95–124. https://doi.org/10.2307/1942161

Seibold, S., Brandl, R., Buse, J., Hothorn, T., Schmidl, J., Thorn, S., & Müller, J. (2015). Association of extinction risk of saproxylic beetles with ecological degradation of forests in Europe. *Conservation Biology*, *29*(2), 382–390. https://doi.org/10.1111/cobi.12427

Seibold, S., Gossner, M. M., Simons, N. K., Blüthgen, N., Müller, J., Ambarlı, D., Ammer, C., Bauhus, J., Fischer, M., Habel, J. C., Linsenmair, K. E., Nauss, T., Penone, C., Prati, D., Schall, P., Schulze, E.-D., Vogt, J., Wöllauer, S., & Weisser, W. W. (2019). Arthropod decline in grasslands and forests is associated with landscape-level drivers. *Nature*, *574*(7780), 671–674. https://doi.org/10.1038/s41586-019-1684-3

Shortall, C. R., Moore, A., Smith, E., Hall, M. J., Woiwod, I. P., & Harrington, R. (2009). Long-term changes in the abundance of flying insects. *Insect Conservation and Diversity*, *2*(4), 251–260. https://doi.org/10.1111/j.1752-4598.2009.00062.x

Sinclair, B. J., Marshall, K. E., Sewell, M. A., Levesque, D. L., Willett, C. S., Slotsbo, S., Dong, Y., Harley, C. D. G., Marshall, D. J., Helmuth, B. S., & Huey, R. B. (2016). Can we predict ectotherm responses to climate change using thermal performance curves and body temperatures? *Ecology Letters*, *19*(11), 1372–1385. https://doi.org/10.1111/ele.12686

Stepanian, P. M., Entrekin, S. A., Wainwright, C. E., Mirkovic, D., Tank, J. L., & Kelly, J. F. (2020). Declines in an abundant aquatic insect, the burrowing mayfly, across major North American

waterways. *Proceedings of the National Academy of Sciences*, *117*(6), 2987–2992. https://doi.org/10.1073/pnas.1913598117

Svenningsen, C. S., Bowler, D. E., Hecker, S., Bladt, J., Grescho, V., Dam, N. M. van, Dauber, J., Eichenberg, D., Ejrnæs, R., Fløjgaard, C., Frenzel, M., Frøslev, T. G., Hansen, A. J., Heilmann-Clausen, J., Huang, Y., Larsen, J. C., Menger, J., Nayan, N. L. B. M., Pedersen, L. B., … Bonn, A. (2020). Contrasting impacts of urban and farmland cover on flying insect biomass. *BioRxiv*, 2020.09.16.299404. https://doi.org/10.1101/2020.09.16.299404

Termaat, T., Strien, A. J. van, Grunsven, R. H. A. van, Knijf, G. D., Bjelke, U., Burbach, K., Conze, K.-J., Goffart, P., Hepper, D., Kalkman, V. J., Motte, G., Prins, M. D., Prunier, F., Sparrow, D., Top, G. G. van den, Vanappelghem, C., Winterholler, M., & WallisDeVries, M. F. (2019). Distribution trends of European dragonflies under climate change. *Diversity and Distributions*, *25*(6), 936–950. https://doi.org/10.1111/ddi.12913

Thorpe, A. S., Barnett, D. T., Elmendorf, S. C., Hinckley, E.-L. S., Hoekman, D., Jones, K. D., LeVan, K. E., Meier, C. L., Stanish, L. F., & Thibault, K. M. (2016). Introduction to the sampling designs of the National Ecological Observatory Network Terrestrial Observation System. *Ecosphere*, *7*(12), e01627. https://doi.org/10.1002/ecs2.1627

Totland, Ö. (1994). Intraseasonal variation in pollination intensity and seed set in an alpine population of Ranunculus acris in southwestern Norway. *Ecography*, *17*(2), 159–165.

van Swaay, C., Dennis, E. B., Schmucki, R., Sevilleja, C., Balalaikins, M., Botham, M., Bourn, N., Brereton, T., Cancela, J. P., Carlisle, B., Chambers, P., Collins, S., Dopagne, C., Escobes, R., Feldmann, R., Fernandez-Gracia, J. M., Fontaine, B., Gracianteparaluceta, A., Harrower, C., … Roy, D. B. (2019). *The EU butterfly indicator for grassland species: 1990-2017*.

Vanbergen, A. J., & Insect Pollinators Initiative. (2013). Threats to an ecosystem service: Pressures on pollinators. *Frontiers in Ecology and the Environment*, *11*(5), 251–259. https://doi.org/10.1890/120126

Wagner, D. L. (2020). Insect declines in the Anthropocene. *Annual Review of Entomology*, *65*(1), 457–480. https://doi.org/10.1146/annurev-ento-011019-025151

Wagner, D. L., Grames, E. M., Forister, M. L., Berenbaum, M. R., & Stopak, D. (2021). Insect decline in the Anthropocene: Death by a thousand cuts. *Proceedings of the National Academy of Sciences*, *118*(2). https://doi.org/10.1073/pnas.2023989118

Warren, R., Price, J., Graham, E., Forstenhaeusler, N., & VanDerWal, J. (2018). The projected effect on insects, vertebrates, and plants of limiting global warming to 1.5°C rather than 2°C. *Science*, *360*(6390), 791–795. https://doi.org/10.1126/science.aar3646

Welti, E. A. R., Kuczynski, L., Marske, K., Sanders, N. J., de Beurs, K. M., & Kaspari, M. (2020). Salty, mild, and low plant biomass grasslands increase top-heaviness of invertebrate trophic pyramids. *Global Ecology and Biogeography*, *29*(9), 1474–1485. https://doi.org/10.1111/GEB.13119

Welti, E. A. R., Roeder, K. A., de Beurs, K. M., Joern, A., & Kaspari, M. (2020). Nutrient dilution and climate cycles underlie declines in a dominant insect herbivore. *Proceedings of the National Academy of Sciences of the United States of America*, *117*(13), 7271–7275. https://doi.org/10.1073/pnas.1920012117

Wepprich, T., R. Adrion, J., Ries, L., Wiedmann, J., & M. Haddad, N. (2019). Butterfly abundance declines over 20 years of systematic monitoring in Ohio, USA. *PLOS ONE*, *14*, e0216270. https://doi.org/10.1371/journal.pone.0216270

Wilson, R. J., & Fox, R. (2020). Insect responses to global change offer signposts for biodiversity and conservation. *Ecological Entomology*, *Early View*. https://doi.org/10.1111/een.12970

Winfree, R., Bartomeus, I., & Cariveau, D. P. (2011). Native pollinators in Anthropogenic habitats. *Annual Review of Ecology, Evolution, and Systematics*, *42*(1), 1–22. https://doi.org/10.1146/annurev-ecolsys-102710-145042

Zuur, A., Ieno, E. N., Walker, N., Saveliev, A. A., & Smith, G. M. (2009). *Mixed effects models and extensions in ecology with R*. Springer-Verlag. https://doi.org/10.1007/978-0-387-87458-6

Supporting Information: Supplemental Tables and Figures for:

Temperature drives variation in flying insect biomass across a German malaise trap network

Contents:

Table S1-S4

Fig. S1-S5

Table S1. Locations of 84 malaise traps and dominant land-cover category.

Location	Latitude	Longitude	Dominant Land-cover
Nationalpark Jasmund_Gumm / 3	54.555368	13.577896	NonIrrigatedCrop
Nationalpark Jasmund_Fahrn / 2	54.546179	13.659444	Forest
Nationalpark Jasmund_Goethe / 1	54.534736	13.655306	Forest
Nationalpark Vorpommersche Boddenlandschaft_DO / 1	54.477017	12.5112	Saltwater
Nationalpark Vorpommersche Boddenlandschaft_Lang / 2	54.441805	12.49133	Forest
Nationalpark Vorpommersche Boddenlandschaft_Heidensee / 3	54.437983	12.49335	Forest
Uni Rostock_ZI	54.42497	12.68462	Freshwater
Uni Greifswald_ELD/02	54.07926	13.476209	NonIrrigatedCrop
Uni Greifswald_ELD/01	54.075671	13.479164	NonIrrigatedCrop
BR Flusslandschaft Elbe MV_Rb_01	53.84217	11.12053	NonIrrigatedCrop
Nationalpark Niedersächsisches Wattenmeer	53.58827096	6.723134972	PastureOrchard
BR Schaalsee_Kb_01	53.464759	10.464053	NonIrrigatedCrop
BR Schaalsee_Db_01	53.335175	11.050982	NonIrrigatedCrop
BR Flusslandschaft Elbe MV	53.204663	11.030898	Forest
Nationalpark Unteres Odertal_AGG	53.130186	14.359659	GrassShrubland
Nationalpark Unteres Odertal_AGU	53.062096	14.323734	GrassShrubland
Leibniz-Institut für Gewässerökologie und Binnenfischerei	52.451228	13.643994	Forest
Nationalpark Harz_NP_Hz_Bu	51.8801	10.6553	Forest
Nationalpark Harz_NP_Hz_Bro	51.7982	10.6174	Forest
Nationalpark Harz_NP_Hz_Fi	51.7924	10.5155	Forest
TERENO_TER_FBG_1	51.622578	11.723798	NonIrrigatedCrop
TERENO_TER_FBG_2	51.62093	11.701777	NonIrrigatedCrop
TERENO_TER_SST_1	51.393613	11.748875	NonIrrigatedCrop
TERENO_TER_SST_2	51.39195	11.703426	NonIrrigatedCrop
Leipziger Auwaldkran_LCC-AWS-01	51.377217	12.280009	Forest
Leipziger Auwaldkran_LCC-AWS-02	51.375858	12.276423	Forest
Leipziger Auwaldkran_LCC-LE	51.367403	12.308824	Forest
BR Oberlausitzer Heide- und Teichlandschaft_TG/3	51.350467	14.664863	Freshwater
BR Oberlausitzer Heide- und Teichlandschaft_GL/1	51.346559	14.575978	PastureOrchard
BR Oberlausitzer Heide- und Teichlandschaft_AL/2	51.34004	14.634769	Forest
Nationalpark Kellerwald-Edersee_NP_Kel_02	51.159	8.93955	Forest
Nationalpark Kellerwald-Edersee_NP_Kel_04	51.15508	8.79752	Forest
Nationalpark Kellerwald-Edersee_NP_Kel_01	51.14229	8.92874	Forest
Nationalpark Kellerwald-Edersee_NP_Kel_03	51.13155	8.97643	Forest
Biodiversitäts-Exploratorium Hainich-Dün_HEG 19	51.073372	10.473357	PastureOrchard
Biodiversitäts-Exploratorium Hainich-Dün_HEW 42	51.06991	10.273537	Forest
Kammeyergarten (HTW Dresden)	51.00973	13.87283	Urban
Nationalpark Eifel_K7	50.60815	6.423185	Forest
Nationalpark Eifel_Lohrbachskopf	50.596079	6.464039	Forest
Nationalpark Eifel_Malsbenden	50.579769	6.467363	Forest
Nationalpark Eifel_Dedenborn	50.569256	6.359577	Forest
Nationalpark Eifel_Klusenberg	50.558923	6.403459	PastureOrchard

Nationalpark Eifel_Müsaulsberg	50.540129	6.380197	GrassShrubland
Rhein-Main-Observatorium_O7 M5	50.32513	9.49509	PastureOrchard
Rhein-Main-Observatorium_S5 M4	50.19838	9.18597	Urban
Rhein-Main-Observatorium_O3 M3	50.18603	9.09684	NonIrrigatedCrop
Rhein-Main-Observatorium_W4 M2	50.18383	9.08732	Forest
Rhein-Main-Observatorium_A1 M6	50.17989	8.95835	NonIrrigatedCrop
Rhein-Main-Observatorium_W2 M1	50.14157	8.98389	Forest
Hammelburg_672/0879	50.10155	9.872025	Forest
Hammelburg_672/0623	50.081017	9.868256	GrassShrubland
Hammelburg_672/0660	50.080042	9.854267	GrassShrubland
Hammelburg_672/0613	50.061344	9.853936	GrassShrubland
Hammelburg_672/0632	50.053814	9.862878	GrassShrubland
Haßfurt-Prappach	50.052633	10.567867	NonIrrigatedCrop
Hammelburg_672/0878	50.051675	9.810758	Forest
Hammelburg_672/0614	50.050261	9.867828	GrassShrubland
Hammelburg_672/0619	50.05	9.857231	GrassShrubland
Zeil-Schmachtenberg	50.004987	10.609725	NonIrrigatedCrop
Ebelsbach-Steinbach	49.998288	10.63084	NonIrrigatedCrop
Ebelsbach_1100/049	49.9814	10.686604	Forest
Ebelsbach_1100/053	49.97884	10.701188	Forest
Bavaria_6029_3For	49.91667	10.52549	Forest
Bavaria_6225_2Urb	49.77293	9.929597	Urban
Nationalpark Hunsrück-Hochwald_Erbeskopf / 4	49.72858	7.094094	Forest
Nationalpark Hunsrück-Hochwald_Wildwiese Thranenweiher / 3	49.7081	7.10412	Forest
Nationalpark Hunsrück-Hochwald_Bunker / 2	49.702007	7.090252	Forest
Nationalpark Hunsrück-Hochwald_Abentheuer / 1	49.652115	7.090571	Forest
Bavaria_6532_3Urb	49.420593	11.050254	Urban
Bavaria_6945_2For	49.08558	13.304759	Forest
Nationalpark Bayerischer Wald_KOL	49.05463	13.2552	Forest
Bavaria_6938_4Urb	49.00426	12.09667	Urban
Nationalpark Bayerischer Wald_BER	48.89879	13.44339	Forest
Nationalpark Schwarzwald_NP_SW_02	48.688465	8.241284	Forest
Nationalpark Schwarzwald_NP_SW_03	48.684751	8.235532	Forest
Bavaria_7544_2Ag	48.583249	13.390587	Urban
Nationalpark Schwarzwald_NP_SW_01	48.510327	8.219127	Forest
Biodiversitäts-Exploratorium Schwäbische Alb_AEG 50	48.405781	9.467762	PastureOrchard
Biodiversitäts-Exploratorium Schwäbische Alb_AEW 06	48.394119	9.446531	Forest
Bavaria_7935_2Urb	48.06033	11.64965	NonIrrigatedCrop
Bavaria_8130_2For	47.87829	10.81209	Forest
Nationalpark Berchtesgaden_Stubenalm 2	47.58952579	12.93652472	Forest
Nationalpark Berchtesgaden_Schapbach 1	47.58526593	12.95199356	Forest
Nationalpark Berchtesgaden	47.57017655	12.95833947	Forest

Table S2. Top AIC models ($\Delta AIC_c<2$) of predictors of flying insect biomass. All models included the random variable of trap identity. Predictor variables are defined in the Methods. Marg R^2= marginal R^2 or the percent variance explained by the fixed effects, Cond R^2= conditional R^2 or the percent variance explained by the fixed effects plus the random effect of trap, df= degrees of freedom, logLik= log likelihood, and w= model weight. For summary tables of model estimates, see Table 1.

Int	elevation	poly (period,2)	tmax	%forest	Marg R^2	Cond R^2	df	logLik	AICc	Δ	w
2.28		+	0.04708	-0.319	0.43	0.73	7	-378.56	771.2	0	0.17
2.21	0.036	+	0.04787	-0.487	0.45	0.73	8	-378.39	772.9	1.7	0.073

Table S3. Model coefficients for the interaction between monthly tmax and Δtemp (Fig. 3). Models were fit for each 2019 sampling month including April (a; $F_{(3,64)} = 13.2$, $R^2 = 0.38$, $P < 0.001$), May (b; $F_{(3,78)} = 6.8$, $R^2 = 0.21$, $P < 0.001$), June (c; $F_{(3,78)} = 14.5$, $R^2 = 0.36$, $P < 0.001$), July (d; $F_{(3,79)} = 15.5$, $R^2 = 0.37$, $P < 0.001$), August (e; $F_{(3,72)} = 5.3$, $R^2 = 0.18$, $P = 0.002$), September (f; $F_{(3,64)} = 5.7$, $R^2 = 0.21$, $P = 0.002$), and October (g; $F_{(3,59)} = 3.1$, $R^2 = 0.14$, $P = 0.03$).

	Estimate	**Stand. Error**	**t-value**	***P***
a) April				
Intercept	0.74	1.42	0.52	0.61
tmax	0.16	0.10	1.53	0.13
Δtemp	0.07	0.70	0.11	0.92
tmax * Δtemp	-0.01	0.05	-0.22	0.83
b) May				
Intercept	0.83	0.76	1.10	0.28
tmax	0.14	0.05	2.81	0.006
Δtemp	-1.17	0.80	-1.46	0.15
tmax * Δtemp	0.07	0.05	1.31	0.19
c) June				
Intercept	-4.19	1.81	-2.31	0.023
tmax	0.30	0.08	4.03	< 0.001
Δtemp	1.51	0.43	3.47	< 0.001
tmax * Δtemp	-0.06	0.02	-3.28	< 0.001
d) July				
Intercept	-4.11	1.38	-2.99	0.004
tmax	0.32	0.06	5.36	< 0.001
Δtemp	2.87	0.71	4.05	< 0.001
tmax * Δtemp	-0.12	0.03	-3.94	< 0.001
e) August				
Intercept	0.32	4.92	0.06	0.95
tmax	0.13	0.20	0.67	0.50
Δtemp	0.13	1.75	0.08	0.94
tmax * Δtemp	-0.01	0.07	-0.16	0.88
f) September				
Intercept	-1.25	1.61	-0.78	0.44
tmax	0.23	0.09	2.58	0.012
Δtemp	1.93	2.25	0.85	0.40
tmax * Δtemp	-0.12	0.13	-0.95	0.35
g) October				
Intercept	1.81	1.75	1.03	0.31
tmax	0.06	0.13	0.46	0.64
Δtemp	-0.66	1.13	-0.59	0.56
tmax * Δtemp	0.04	0.08	0.51	0.61

Table S4. Top models ($\Delta AIC_c < 2$) for day of peak flying insect biomass. Predictor variables are defined in the Methods. Df= degrees of freedom, logLik= log likelihood, and w= model weight.

Intercept	elevation	precip	Δtemp	%forest	%grassland /shrubland	%pasture /orchard	%urban	R^2	df	logLik	AICc	ΔAICc	w
183.1					-20.85			0.07	3	-291.94	590.2	0	0.03
180.9					-19.1	14.66		0.09	4	-290.87	590.3	0.12	0.028
174.4	-1.93	2.41			-21.83			0.11	5	-289.96	590.8	0.59	0.022
171.6	-1.83	2.46			-20.37	14.35		0.13	6	-288.92	591.1	0.9	0.019
193.5			-5.01		-21.66			0.08	4	-291.31	591.2	0.98	0.018
185.1				-4.13	-22.29			0.08	4	-291.51	591.6	1.39	0.015
190.2			-4.40		-19.94	13.65		0.1	5	-290.38	591.7	1.44	0.015
184.7	-1.84	2.61	-5.72		-23.25			0.13	6	-289.22	591.7	1.49	0.014
184.2	-0.32				-20.29			0.07	4	-291.72	592	1.8	0.012
175	-1.75	2.64		-5.49	-24.47			0.12	6	-289.44	592.1	1.92	0.011
181.6	-1.75	2.64	-5.48		-21.78	13.92		0.14	7	-288.22	592.2	1.95	0.011
182.6					-19.9		5.41	0.07	4	-291.80	592.2	1.97	0.011

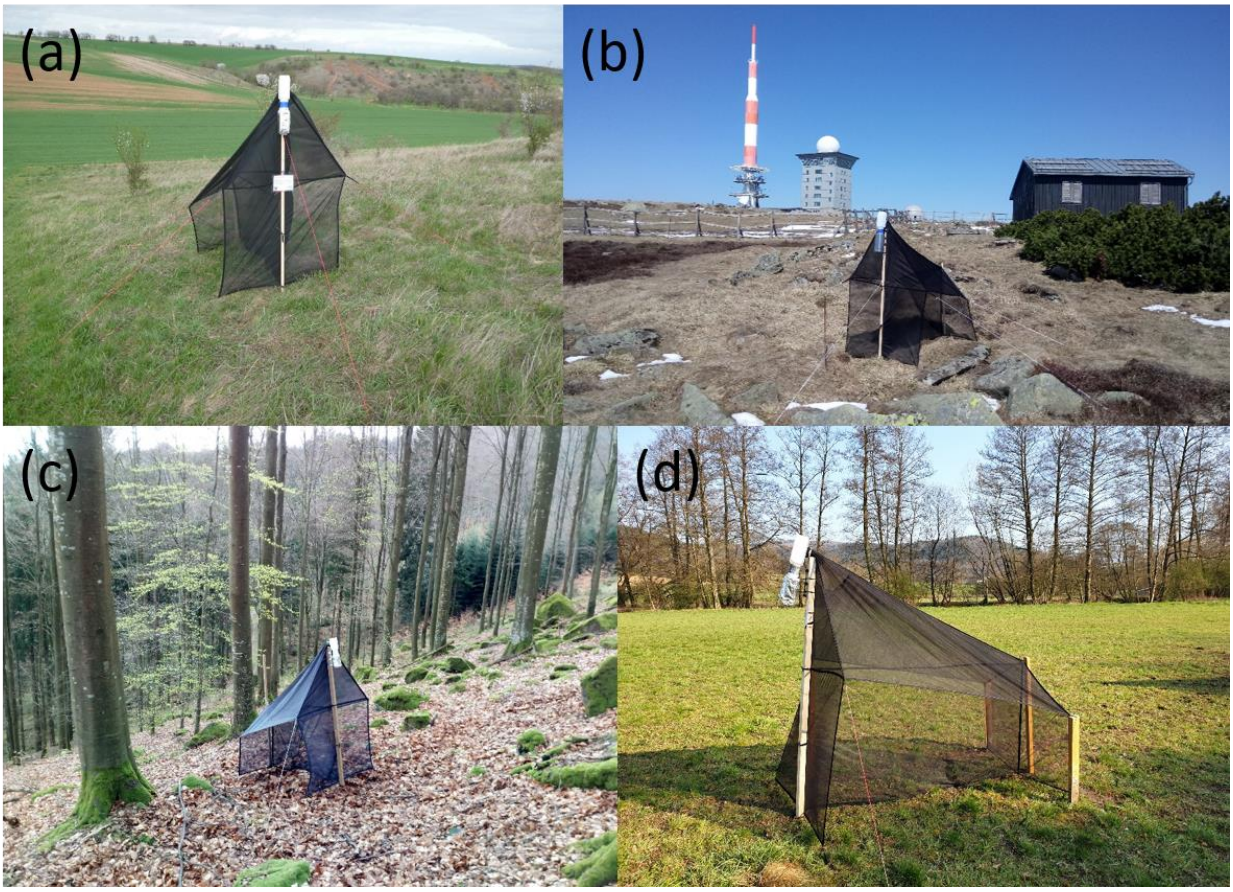

Figure S1. Examples of traps running in 2019 as part of the German Malaise Trap Program. Photos show traps at the LTER site Tereno- Friedeburg (a; photo credit: Mark Frenzel), at the Harz National Park (b; photo credit: Andreas Marten), at the Black Forest National Park (c; photo credit: Jörn Buse), and at the LTER site Rhine-Main-Observatory (d; photo credit: Peter Haase).

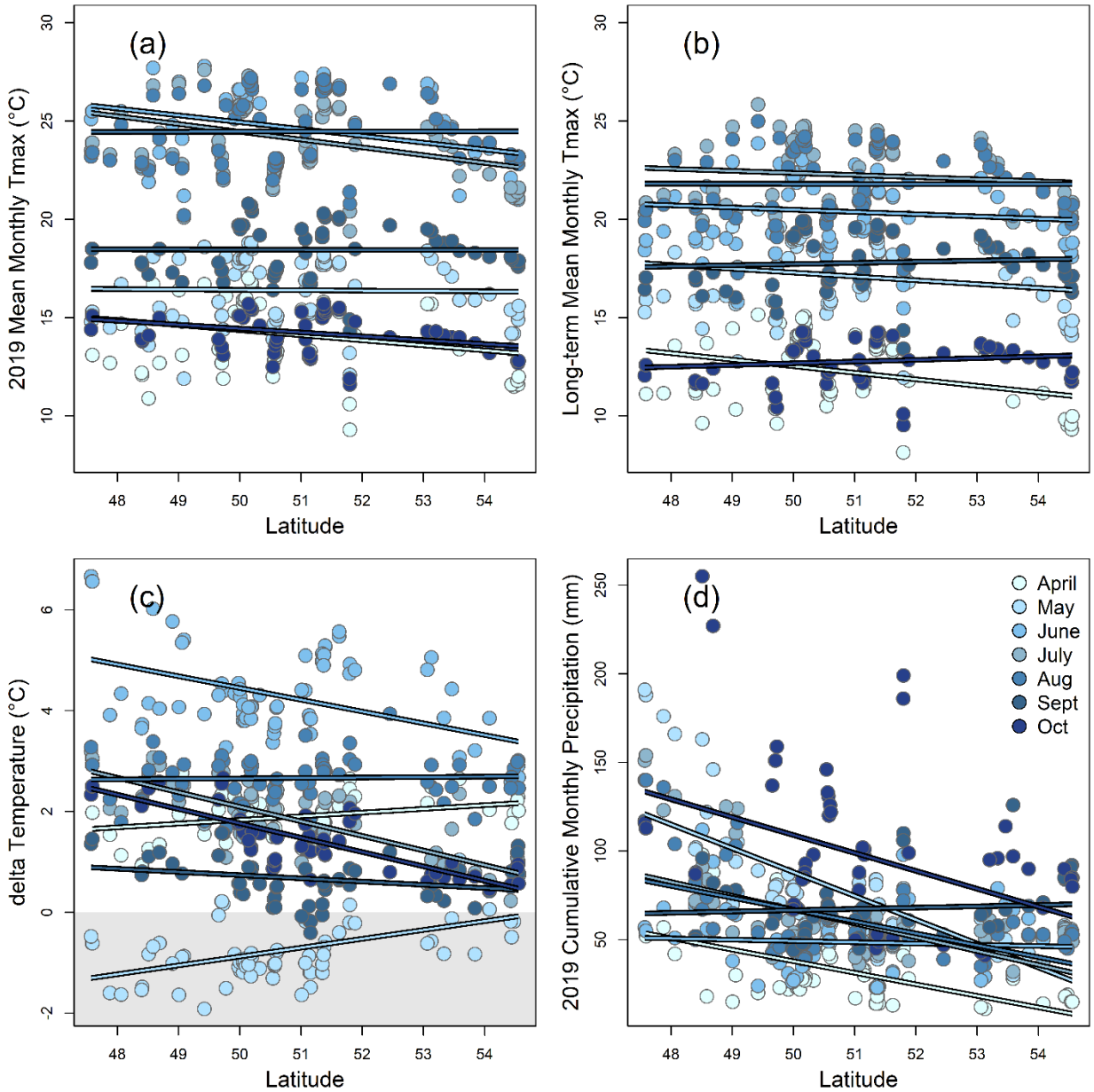

Figure S2. Changes with latitude across our 84 trap locations in 2019 mean monthly maximum temperature (a), the 1960-2018 long-term average monthly maximum temperature (b), the change in 2019 mean monthly maximum temperature minus the 1960-2018 long-term average (c), and 2019 cumulative monthly precipitation (d). Each point represents one month at one location, and only month/location combinations from which flying insect biomass data were collected are included. Averaging across April to October, 2019 mean monthly maximum temperature showed a weak trend to decrease with latitude (a; $F_{1,82} = 2.7$, $R^2 = 0.03$, $P = 0.10$), while the 1960-2018 long-term average monthly maximum temperature did not vary with latitude (b; $F_{1,82} = 0.6$, $R^2 < 0.01$, $P = 0.44$). While varying with month, the average Δ °C of 2019 maximum temperature over the long-term average decreased with latitude (c; $F_{1,82} = 12.6$, $R^2 = 0.13$, $P < 0.001$), as did cumulative monthly precipitation (d; $F_{1,82} = 26.8$, $R^2 = 0.24$, $P < 0.001$).

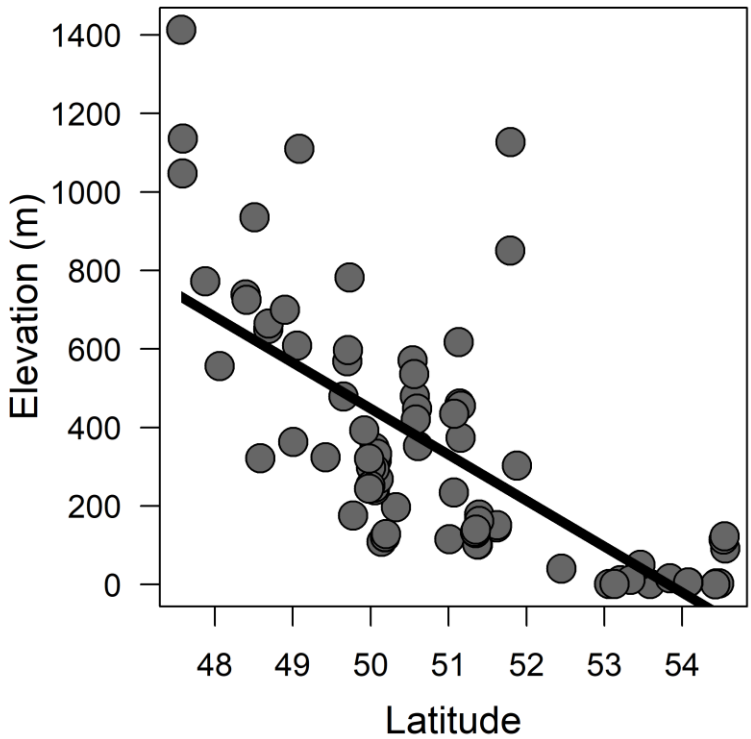

Figure S3. Elevation declined with increasing latitude across our 84 trap locations ($F_{1,82} = 74.5$, $R^2 = 0.48$, $P < 0.001$).

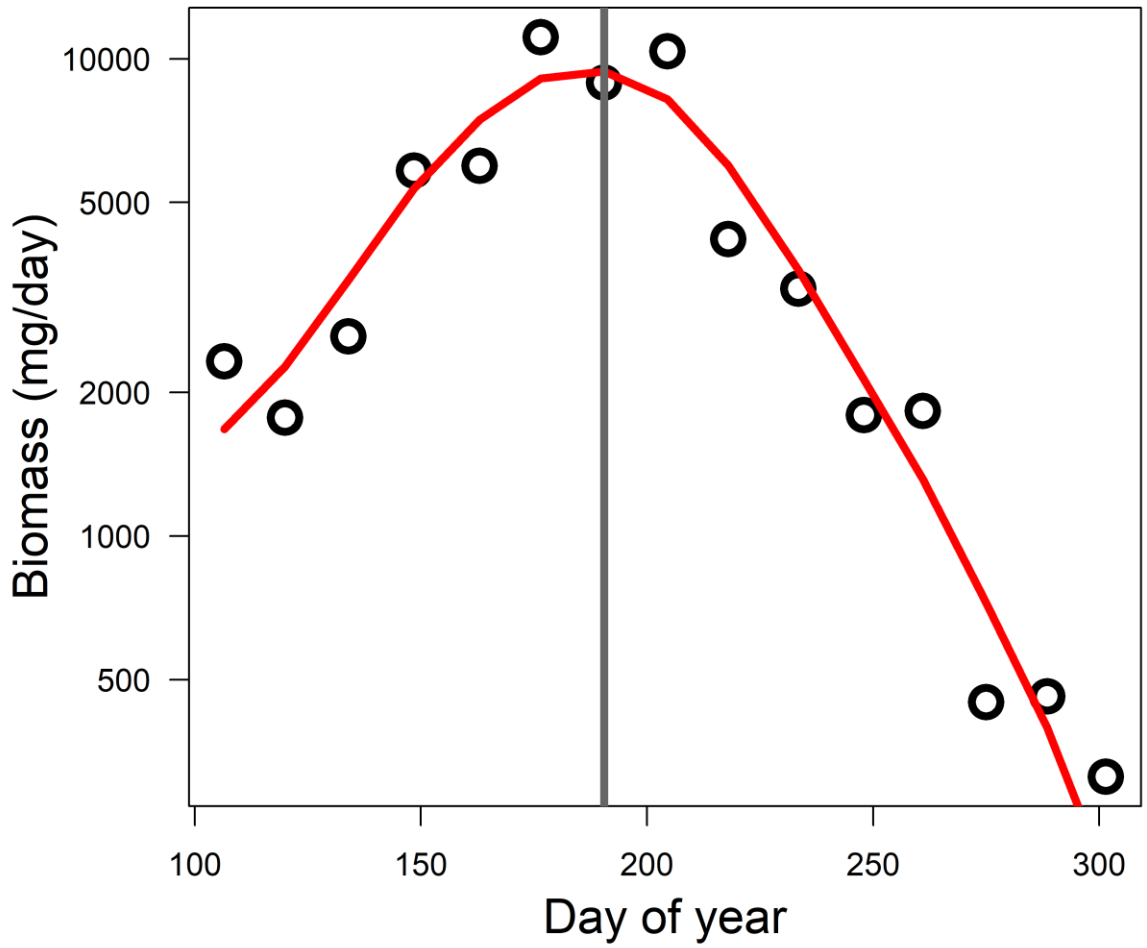

Figure S4. Example of determination of peak biomass day from a trap at Hunsrück-Hochwald National Park. Points represent the biomass (mg/day) collected from each sample plotted over the median day of the year of the sample. The red line is a spline fitted to these points. The grey vertical line show the maximum value of the spline, at which the day of year was extracted. At this site, 2019 peak biomass was estimated to occur at the 190.5th day of the year (July 9th-10th).

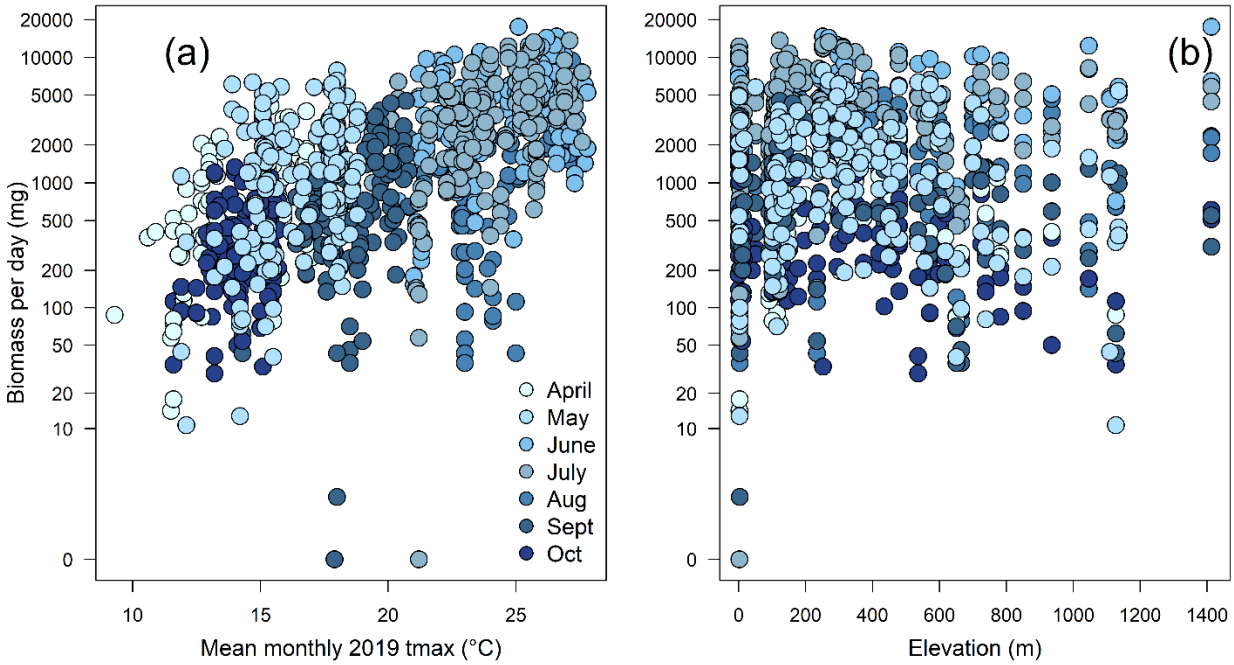

Figure S5. Responses of flying insect biomass to tmax and elevation. Each point represents the biomass from one sample. Across all months and site combinations, flying insect biomass increased with mean monthly 2019 maximum temperature (a), and increased weakly with elevation (b). Model estimates are provided in Table 1.